Monthly Notices
of the
ROYAL ASTRONOMICAL SOCIETY

MNRAS **485,** 3715–3720 (2019)
Advance Access publication 2019 March 02

doi:10.1093/mnras/stz607

The ultracool helium-atmosphere white dwarf companion of PSR J0740+6620?

D. M. Beronya [1★], A. V. Karpova [1★], A. Yu. Kirichenko [2,1], S. V. Zharikov,[2] D. A. Zyuzin [1], Yu. A. Shibanov[1,3] and A. Cabrera-Lavers[4,5]

[1]*Ioffe Institute, Politekhnicheskaya 26, St. Petersburg 194021, Russia*
[2]*Instituto de Astronomía, Universidad Nacional Autónoma de México, Apdo. Postal 877, Baja California, México 22800, Mexico*
[3]*Peter the Great St. Petersburg Polytechnic University, Politekhnicheskaya 29, St. Petersburg 195251, Russia*
[4]*GRANTECAN, Cuesta de San José s/n, E-38712, Breña Baja, La Palma, Spain*
[5]*Instituto de Astrofísica de Canarias, Vía Láctea s/n, E-38200, La Laguna, Tenerife, Spain*

Accepted 2019 February 26. Received 2019 February 22; in original form 2018 December 5

ABSTRACT

We report detection of the likely companion of the binary millisecond pulsar (MSP) J0740+6620 with the Gran Telescopio Canarias in the r' and i' bands. The position of the detected starlike source coincides with the pulsar coordinates within the 1σ uncertainty of $\approx$0.2 arcsec. Its magnitudes are $r' = 26.51 \pm 0.17$ and $i' = 25.49 \pm 0.15$. Comparing the data with the white dwarf (WD) cooling tracks suggests that it can be an ultracool helium-atmosphere WD with the temperature $\lesssim$3500 K and cooling age $\gtrsim$5 Gyr. The age is consistent with the pulsar characteristic age corrected for kinematic effects. This is the reddest source among known WD companions of MSPs. Detection of the source in other bands would be useful to clarify its properties and nature.

Key words: stars: neutron – pulsars: general – binaries: general – pulsars: individual: PSR J0740+6620.

1 INTRODUCTION

Millisecond pulsars (MSPs) are neutron stars (NSs) with short rotation periods P, typically below 30 ms. They have small spin-down rates ($\dot{P} \lesssim 10^{-19}$ s s^{-1}) and constitute a special subclass on the P–$\dot{P}$ diagram, distinct from the population of 'normal' pulsars (e.g. Manchester 2017a). The first MSP, PSR B1937+21, was discovered in 1982 (Backer et al. 1982). It is believed that these objects are formed in binary systems: the initially more massive of the two binary components star turns into a NS that is then spun-up (or 'recycled') due to accretion of matter from the secondary star (Bisnovatyi-Kogan & Komberg 1974; Alpar et al. 1982; Tauris 2011). This is supported by the fact that a high (>50 per cent) fraction of MSPs has companions and by discoveries of several MSPs switching between the rotation-powered and accretion-powered pulsar states (Archibald et al. 2009; Papitto et al. 2013; Bassa et al. 2014; Roy et al. 2015). Moreover, the NS binary 1FGL J1417.7−4402 was recently found to be in the late stages of the canonical MSP recycling process (see Swihart et al. 2018, and references therein).

Spin periods of MSPs are extraordinarily stable that may be related to their weak external magnetic fields (Manchester 2017a). The period stability makes MSPs important in different areas of astrophysics. For instance, studies of the binary pulsar PSR B1913+16, the double-pulsar system PSR J0737−3039A/B and especially the triple system PSR J0337+1715 allow one to carry out unprecedented tests of general relativity (Weisberg & Huang 2016; Archibald et al. 2018; Kramer 2018, and references therein). A set of MSPs (or 'Pulsar Timing Array') was proposed for detection of low-frequency gravitational waves and spacecraft navigation (Manchester 2017b; Becker, Kramer & Sesana 2018). MSP timing is also used to obtain physical characteristics of stellar clusters (Freire et al. 2017; Prager et al. 2017). Studies of MSPs are essential for exploration of binary and stellar evolution and also reveal properties of the interstellar medium (ISM). Binary systems containing an MSP allow for most accurate determination of NSs masses that play a key role in constraints on equation of state (EoS) of the superdense matter in NSs interiors (Lattimer 2012; Antoniadis et al. 2013).

In a binary system masses of both the NS and its companion can be inferred with a high precision through the measurement of the general relativistic Shapiro delay from pulsar radio timing observations (Shapiro 1964; Jacoby et al. 2005). However, the effect is strong for edge-on systems; otherwise, additional optical observations are necessary. The latter are also crucial for determination of an MSP companion nature (e.g. van Kerkwijk et al. 2005). Low-mass white dwarfs (WDs) are the most frequent MSP companions (Tauris 2011). In such a case, comparison between the optical data and WD evolutionary sequences can provide the type, temperature,

★ E-mail: daria.beronya@gmail.com (DMB);
annakarpova1989@gmail.com (AVK)

Table 1. Parameters of the J0740 system (from Arzoumanian et al. 2018). Current values are available in the NANOGrav Data Repository.[a] The dispersion measure distances $D_{\rm YMW}$ and $D_{\rm NE2001}$ were estimated using the YMW16 (Yao, Manchester & Wang 2017) and NE2001 (Cordes & Lazio 2002) models for the distribution of free electrons in the Galaxy, respectively. The distance $D_{\rm p}$ corresponds to the timing parallax of 2.3(6) mas. Numbers in parentheses are 1σ uncertainties related to the last significant digits quoted.

Right ascension α (J2000)	$07^{\rm h}40^{\rm m}45\overset{\rm s}{.}79492(2)$
Declination δ(J2000)	$+\,66^\circ20'33\overset{''}{.}5593(2)$
Galactic longitude l (deg)	149.7
Galactic latitude b (deg)	29.6
Epoch (MJD)	57017
Proper motion $\mu_\alpha = \dot{\alpha}\cos\delta$ (mas yr^{-1})	−10.3(2)
Proper motion μ_δ (mas yr^{-1})	−31.0(2)
Spin period P (ms)	2.885 736 410 850 19(2)
Period derivative $\dot{P}$ (10^{-20} s s^{-1})	1.2184(4)
Characteristic age τ (Gyr)	3.75
Spin-down luminosity $\dot{E}$ (erg s^{-1})	2.0×10^{34}
Orbital period $P_{\rm b}$ (d)	4.766 944 619(1)
Projected semimajor axis (lt-s)	3.977 5602(2)
Eccentricity (10^{-6})	4.9(1)
Mass function $f_{\rm M}$ ($M_\odot$)[b]	0.003
Minimum companion mass $M_{\rm c,min}$ ($M_\odot$)[b]	0.2
Dispersion measure (DM, pc cm^{-3})	15.0
Distance $D_{\rm YMW}$ (kpc)	0.93
Distance $D_{\rm NE2001}$ (kpc)	0.68
Distance $D_{\rm p}$ (kpc)	$0.4^{+0.2}_{-0.1}$

[a] https://data.nanograv.org/

[b] Parameters are provided by Lynch et al. (2018). $M_{\rm c,min}$ is calculated assuming the inclination angle $i = 90$ deg and the pulsar mass $M_{\rm p} = 1.4\,M_\odot$.

Table 2. Log of the GTC observations. The mean airmass and seeing values are presented.

Filter	Exposure time (s)	Airmass	Seeing (arcsec)
r'	15 × 1	1.32	0.9
	120 × 31	1.29	0.9
i'	15 × 1	1.26	0.8
	120 × 20	1.26	0.8

cooling age, and mass of the WD. Knowing the companion mass, the mass function (from pulsar timing observations) and the mass ratio (from the optical phase-resolved spectroscopy), one can estimate the pulsar mass and the system inclination. Unfortunately, due to the weakness of the optical counterparts, identifications of MSP companions are not numerous. Nevertheless, increasing the number of such identifications is important for understanding the nature and origin of these systems. The situation has been improving thanks to the world's largest telescopes and deep sky surveys (e.g. Bassa et al. 2016; Dai et al. 2017; Karpova et al. 2018; Kirichenko et al. 2018).

The subject of this paper, the binary MSP J0740+6620 (hereafter J0740), was discovered in the radio in the frame of the Green Bank North Celestial Cap Pulsar Survey (Stovall et al. 2014; Lynch et al. 2018). The pulsar was also identified in gamma-rays with the *Fermi* telescope (Laffon et al. 2015; Guillemot et al. 2016). Table 1 summarizes the parameters of the pulsar system. Based on the computed minimum companion mass of ≈0.2 $M_\odot$, Lynch et al. (2018) suggested that the pulsar companion is a He WD. Using the magnitude lower limits from the PanSTARRS 3π Steradian Survey bands, they constrained the WD temperature <4200 K and age >3.2 Gyr.

To find the optical counterpart of the pulsar companion, we performed deep optical observations with the Gran Telescopio Canarias (GTC). Here, we report a likely identification of the pulsar companion. The details of the observations and data reduction are described in Section 2, the analysis and results are presented in Section 3 and discussed in Section 4.

2 OBSERVATIONS AND DATA REDUCTION

The observations of the J0740 field were performed on 2017 December 26[1] in the Sloan r' and i' bands using the GTC/OSIRIS[2] instrument. The conditions were photometric and seeing varied from 0.8 to 1.3 arcsec. The instrument field of view (FOV) was 7.8 arcmin × 7.8 arcmin with the pixel scale of 0.254 arcsec. The pulsar was exposed on the CCD2 chip of the two OSIRIS CCD chips. The dithered science frames of 120 s were taken, resulting in the total exposure times of 3.7 and 2.4 ks for the r' and i' filters, respectively. The short 15 s exposures were obtained in each band to avoid saturation of bright stars that were further used for precise astrometry. The observing log is presented in Table 2.

The data reduction and analysis were carried out within the Image Reduction and Analysis Facility (IRAF) package. The raw data included 10 bias frames and 5 sky flats for each filter, which were used to create the master bias and master flats frames. The bias subtracted and the flat-fielded science frames were obtained with the CCDPROC routine, aligned to the frame with the best seeing, and then stacked for each filter using the IMCOMBINE task. Accounting for known OSIRIS geometrical distortions and background gradients in the images towards the FOV boundaries,[3] we ignored the areas outside 2.5 arcmin from the target to avoid the influence of these effects on the calibration and further results.

To perform the astrometric transformation, we used the IRAF CCMAP task and nine bright non-saturated reference stars detected with a high signal-to-noise ratio in the r'-band short-exposure frame. The best coordinates of the stars are contained in the *Gaia* DR2 catalogue (Gaia Collaboration 2016, 2018) and have the catalogue conservative accuracy of ≈0.7 mas (Lindegren et al. 2018). The resulting 1σ *rms* uncertainties of the astrometric fit are 0.08 arcsec in RA and Dec. The *Gaia* catalogue uncertainties are substantially smaller and can be neglected. The resulting WCS solution was applied to the combined images in the r' and i' bands. Selecting other reference stars did not change the fit result.

For the photometric calibration, we used the Landolt standard star G163-50 (Landolt 1992) observed during the same night as the target. The derived photometric zero-points for the CCD2 chip are $z_{r'} = 28.88 \pm 0.01$ and $z_{i'} = 28.52 \pm 0.02$. The values were obtained by comparing the standard star magnitudes from Smith et al. (2002) with its instrumental magnitudes, corrected for the finite aperture and atmospheric extinction. We used the atmospheric extinction coefficients[4] $k_{r'} = 0.07 \pm 0.01$ and $k_{i'} = 0.04 \pm 0.01$. The 3σ detection limits on the resulting images are $r' < 27.5$ and $i' < 26.5$.

[1] Proposal GTCMULTIPLE2A-17BMEX, PI A. Kirichenko

[2] http://www.gtc.iac.es/instruments/osiris/

[3] http://www.gtc.iac.es/instruments/osiris/media/OSIRIS-USER-MANUAL_v3_1.pdf

[4] http://www.iac.es/adjuntos/cups/CUps2014-3.pdf

3 RESULTS

Fig. 1 shows the sections of the r' and i' images, containing the J0740 position. The radio coordinates of the pulsar corrected for the proper motion (Table 1) to the epoch of our observations (58114 MJD) are RA = $07^h40^m45\overset{s}{.}7898(1)$ and Dec. = $+66°20'33\overset{''}{.}4661(6)$. Accounting for the astrometric referencing uncertainty, the radius of the J0740 1σ position error circle on the optical images is ≈0.08 arcsec. In the main panels of Fig. 1, we show the 3σ circle for convenience. A faint starlike source is detected in both bands, which overlaps with the circle. Its coordinates RA = $07^h40^m45\overset{s}{.}76(1)$ and Dec. = $+66°20'33\overset{''}{.}4(2)$ were derived as a mean of the source positions in both bands. The errors account for the position uncertainties of the object in the frames, the difference in the positions in the two bands, and the astrometric referencing uncertainty. The object coordinates coincide with the pulsar position at the 1σ significance level. This is demonstrated in the inset of the right-hand panel of Fig. 1 where the 1σ position circles for the pulsar and the object overlap.

For photometry of this faint object, we used the circular source aperture with ≈0.76 arcsec (3 pixels) radius, which is consistent with the seeing value and provides the maximum signal-to-noise ratio on the source. To minimize possible contributions from wings of nearby sources, backgrounds were taken from a narrow annulus centred on the source with the inner and outer radii of ≈ 0.8 and 1.5 arcsec. As a result, we obtained the source magnitudes $r' = 26.51 \pm 0.17$ and $i' = 25.49 \pm 0.15$ corrected for the finite aperture and the atmospheric extinction. Alternatively, for both bands we constructed the point spread functions (PSFs) using about a dozen of unsaturated isolated field stars and the DAOPHOT package, and performed the PSF-fitting photometry of field sources applying the ALLSTAR routine with the same source aperture but a wider background annulus with the inner and outer radii of ≈ 2.5 and 5 arcsec.[5] This yielded the same object magnitudes with only marginally smaller errors. Our object is perfectly PSF-subtracted without any residuals that could indicate a possible presence of fainter sources hidden in its profile. Finally, we performed the aperture photometry on the images where all neighbours, excluding the object of interest, were PSF-subtracted. Independently of the annulus width this led again to the results consistent with the above aperture and PSF magnitude measurements. We thus adopt the above values as the most conservative ones.

We estimated the probability of detecting a random object at the pulsar position using the Poisson distribution $P = 1 - \exp(-\sigma S)$, where σ is the surface number density of objects within the GTC FOV and S is the area of the pulsar error ellipse. As a result, we found the probability of $\approx 2 \times 10^{-3}$ for an accidental coincidence of the pulsar and an unrelated object with a brightness of >20 mag. This indicates the source is a likely optical counterpart to the J0740 binary companion.

To obtain intrinsic colours and magnitudes of the presumed companion we used the empirical correlation between the distance D and the interstellar reddening $E(B-V)$ based on the Pan-STARRS 1 and 2MASS photometric data (Green et al. 2018). The expected $E(B-V)$ in the pulsar direction is ≈0.04 ± 0.02 for the most conservative distance range of 0.3–0.9 kpc following from Table 1. This value was transformed to the extinction correction values $A_{r'} = 0.09 \pm 0.05$ and $A_{i'} = 0.07 \pm 0.03$ using the conversion coefficients presented by Schlafly & Finkbeiner (2011). The resulting intrinsic magnitudes and colour index are $r'_0 = 26.42 \pm 0.18$, $i'_0 = 25.42 \pm 0.15$, and $(r' - i')_0 = 1.0 \pm 0.2$, where the errors include uncertainties of the reddening and magnitude measurements. For the above distance range, the absolute magnitude $M_{r'}$ varies from 16.4 to 19.2. The specific values for the timing parallax distance and for the maximum model depended DM distance of 930 pc are $M_{r'} = 18.4^{+0.8}_{-1.1}$ and $16.6^{+0.2}_{-0.2}$, respectively.

As it has been suggested, the J0740 companion is a WD (Lynch et al. 2018). Therefore, we compared the derived colour and magnitudes of the likely companion with the cooling sequences of hydrogen (DA) and helium (DB) WDs. The corresponding colour–magnitude and colour–colour diagrams are presented in Figs 2 and 3, respectively. Cooling tracks for WDs with hydrogen and helium atmospheres (known as Bergeron models: Holberg & Bergeron 2006; Kowalski & Saumon 2006; Bergeron et al. 2011; Tremblay, Bergeron & Gianninas 2011) are shown by different line types.[6] The data points of companions to some other MSPs are presented: J0348+0432 (Antoniadis et al. 2013), J0614−3329 (Bassa et al. 2016), J0621+2514 (Karpova et al. 2018), J0751+1807 (Bassa, van Kerkwijk & Kulkarni 2006), J1012+5307 (Nicastro et al. 1995), J1231−1411 (Bassa et al. 2016), and J2317+1439 (Dai et al. 2017). We also include two ultracool isolated WDs: SDSS J110217.48+411315.4 (hereafter WD J1102; Hall et al. 2008; Kilic et al. 2012) and WD 0346+246 (Oppenheimer et al. 2001). For WD 0346+246 and the PSR J0751+1807 companion, the *UBVRI* magnitudes were converted to the Sloan Digital Sky Survey (SDSS) system using transformations by Lupton.[7] The magnitudes of other objects were adopted either from the cited articles or the SDSS catalogue (Abolfathi et al. 2018). The corresponding values of interstellar reddening $E(B-V)$ of the sources were obtained using the models by Drimmel, Cabrera-Lavers & López-Corredoira (2003), and Green et al. (2018) together with the distances from DM and parallax measurements or model-predicted WD distances. For PSR J2317+1439, the parallax information was updated by Arzoumanian et al. (2018), and for this reason the reddening and absolute magnitude from Dai et al. (2017) were recalculated. For PSR J0621+2514, we combined the results for two DM distance estimates (Karpova et al. 2018).

The J0740 presumed companion is the reddest among sources shown in the diagrams (Figs 2 and 3). The Bergeron models presented here are constructed for CO-core WDs. However, it is generally believed that most of the MSP companions are He-core WDs, due to stripping a companion envelope during the mass-transfer binary phase (see e.g. Cadelano et al. 2015; Rivera-Sandoval et al. 2015). For hydrogen-atmosphere WDs, the comparison of the Bergeron models with those of the He-core ones created by Althaus, Miller Bertolami & Córsico (2013) shows that the presumed J0740 companion cannot certainly belong to DA WDs, considering any core composition. This is because the upper limit for $(r' - i')_0$ indices of the hydrogen atmosphere sequences is $\lesssim 0.5$ for both core types and all DA tracks turn towards blue colours at high ($M_{r'} \gtrsim 16$) absolute magnitudes/low temperatures (see also Bassa et al. 2016). At the same time, the colour index of the presumed companion is about one (Fig. 2). On the other hand, for cool WDs with pure helium atmospheres colours continue to redden with decreasing temperatures. Unfortunately, we have not found respective He-core magnitude sequences for these WDs.

[5]The latter is appropriate as the routine iteratively subtracts brighter neighbours in a source group before the photometry of fainter ones.

[6]http://www.astro.umontreal.ca/~bergeron/CoolingModels

[7]https://www.sdss.org/dr14/algorithms/sdssUBVRITransform/

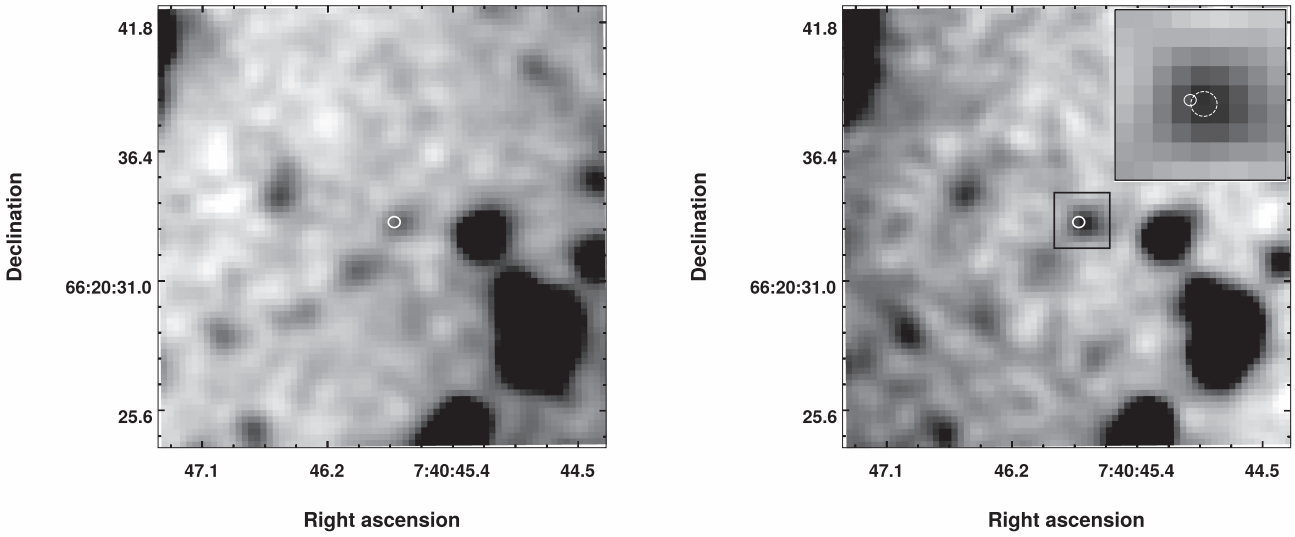

Figure 1. 16 arcsec × 16 arcsec GTC/OSIRIS Sloan r'-band (left) and i'-band (right) images of the J0740 field. The images are smoothed with the Gaussian kernel of 3 pixels, compatible with the seeing value. The white circle shows the 3σ pulsar position uncertainty of ≈0.24 arcsec, which accounts for the optical astrometric referencing errors and the radio timing position uncertainties, corrected for the proper motion. The region of 2.3 arcsec × 2.3 arcsec within the black box in the right-hand panel is enlarged and shown in the inset at the right-top corner of the image. The solid and dashed circles are 1σ position uncertainties of the pulsar and its possible binary companion, respectively.

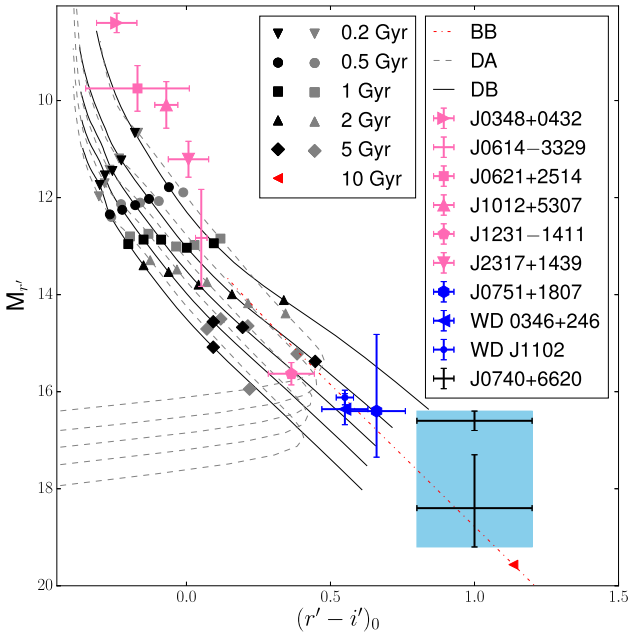

Figure 2. Colour–magnitude diagram with various WD evolutionary sequences and the data for different WDs listed in the legend. Dashed grey and black solid lines show the cooling tracks for WDs with hydrogen (DA) and helium (DB) atmospheres, respectively (Holberg & Bergeron 2006; Kowalski & Saumon 2006; Bergeron et al. 2011; Tremblay et al. 2011) with masses 0.2–1.0 $M_\odot$ (spaced by 0.2 $M_\odot$) increasing from upper to lower curves. Cooling ages are indicated by different symbols. The dash–dotted red line demonstrates the track for a WD with the mass of 0.4 $M_\odot$ emitting the BB spectrum. The location of the J0740 presumed companion is marked by the black crosses: the upper one ($M_{r'} = 16.6^{+0.2}_{-0.2}$) is for the maximum distance estimate $D_{\rm YMW} = 0.93$ kpc and the lower one ($M_{r'} = 18.4^{+0.8}_{-1.1}$) is for the minimum distance estimate $D_{\rm p} = 0.4^{+0.2}_{-0.1}$ kpc, derived from the timing parallax. The light-blue rectangle encompasses the whole distance uncertainty range. The data points for WDs that likely have pure helium or mixed atmospheres are shown in blue.

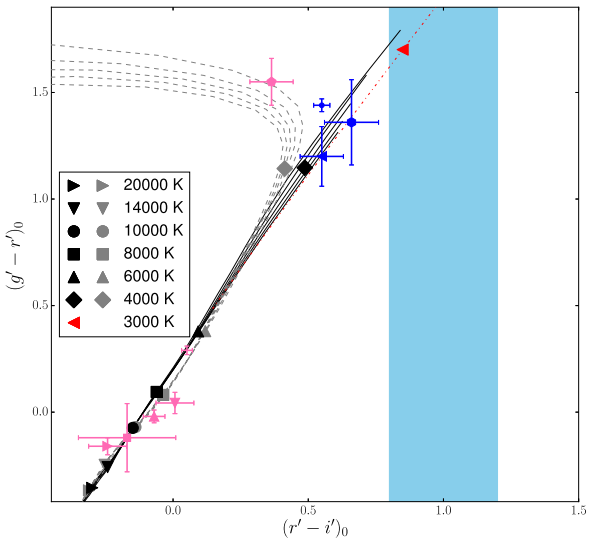

Figure 3. Colour–colour diagram with various WD evolutionary sequences and the data for the same WDs as in Fig. 2. The model predictions presented in Fig. 2 are labelled by the same symbols and colours. WD temperatures are indicated by different symbols. The location range of the likely J0740 companion is shown by the light-blue stripe.

Nevertheless, calculations show that the luminosity of a He-core WD at a given age has to be significantly higher than that of the CO-core WD with the same mass (e.g. van Oirschot et al. 2014). This is due to the fact that the global specific heat capacity of the former is larger than that of the latter. However, at ages $\gtrsim 1$ Gyr the luminosity difference for low-mass WDs becomes less than a half of magnitude that could not be resolved within a factor of 4 larger intrinsic magnitude uncertainty of the presumed companion. This is mainly caused by the large distance uncertainty (light-blue rectangle in Fig. 2). Moreover, the spectral energy distributions of cool helium-atmosphere WDs become close to those of blackbodies

(BBs) (e.g. Kilic 2011). As an example, in the diagrams we present the cooling sequence for a 0.4 $M_\odot$ WD with the BB spectrum, describing the cooling from 6000 to 2000 K. One can see that the presumed J0740 companion position in the diagrams is in agreement with this track. Therefore, it most likely belongs to the class of ultracool WDs with helium atmospheres and has a temperature of $\lesssim$3500 K and a cooling age of $\gtrsim$5 Gyr.

4 DISCUSSION AND CONCLUSIONS

We detected the likely companion to the MSP J0740. The comparison of the photometry results with the WD evolutionary sequences showed that the source is most probably an ultracool WD with a pure helium atmosphere. It can be the reddest WD among the known MSP companions. The WD core composition remains unclear due to the large distance and magnitude uncertainties.

The presumed WD cooling age is $\gtrsim$5 Gyr. If it has a low mass, this age limit can be larger since after the Roche lobe detachment a proto-WD goes through the contraction phase until it reaches its cooling track (Istrate et al. 2014, 2016). The duration of this phase increases as the mass of the proto-WD decreases, and may last as long as ∼2 Gyr. The J0740 characteristic age of 3.75 Gyr (Table 1) is smaller than the WD age estimate. However, the observed pulsar period derivative and consequently its characteristic age can be biased by kinematic effects, i.e. the effects of the pulsar proper motion (Shklovskii effect; Shklovskii 1970), the acceleration towards the Galactic plane and the acceleration due to differential Galactic rotation (Nice & Taylor 1995). Using the J0740 proper motion value from Table 1, the Sun's Galactocentric velocity and the distance (240 km s^{-1} and 8.34 kpc, respectively; Reid et al. 2014), we calculated these corrections to the pulsar period derivative: $\dot{P}_{\rm S} = 3.0 \times 10^{-21}$, $\dot{P}_{\rm G,\perp} = -1.6 \times 10^{-22}$, $\dot{P}_{\rm G,p} = 3.8 \times 10^{-23}$ for the minimum and $\dot{P}_{\rm S} = 6.9 \times 10^{-21}$, $\dot{P}_{\rm G,\perp} = -2.2 \times 10^{-22}$, $\dot{P}_{\rm G,p} = 8.9 \times 10^{-23}$ for the maximum pulsar distance estimates. The corresponding intrinsic characteristic ages are $\tau_i \sim 5$ and ∼8.5 Gyr, which are compatible with the cooling age.[8] Thus, the considered binary system indeed can be very old and the presumed WD can be ultracool. This is not a unique situation. There are other examples of the objects with similar characteristics. One of them is the WD companion of PSR J0751+1807 (Bassa et al. 2006). Its colours (see Figs 2 and 3) indicate that the WD has a pure helium or mixed H/He atmosphere with a temperature $T \sim$ 3500–4300 K. Other examples are isolated ultracool white dwarfs WD J1102 (Hall et al. 2008; Kilic et al. 2012) and WD 0346+246 (Oppenheimer et al. 2001). These WDs have temperatures of about 3650 and 3300 K, respectively, and are best explained by the mixed atmosphere models (Gianninas et al. 2015).

It is clear that a single colour index is not enough to confidently assert that the source is the optical counterpart of the pulsar companion. Although the probability of the accidental coincidence is low, however, it cannot be excluded. As seen from the colour–magnitude diagram presented in Fig. 4, the presumed companion is not very distinct from the distribution of other stellar sources detected within the GTC FOV. It is located near the red locus of the main-sequence distribution. Below we consider possible alternative interpretations of the source nature.

[8]It is well known that the characteristic age is just an estimate of the pulsar true age and can significantly deviate from it (e.g. Lorimer & Kramer 2012). However, it is usually the only available estimate that is the case of J0740. The pulsar true age can be even larger than τ_i if the braking index is <3.

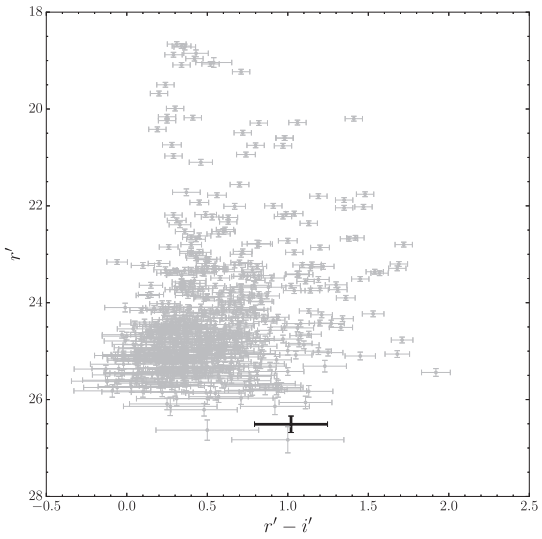

Figure 4. Observed colour–magnitude diagram for about 600 stellar sources in the J0740 field based on the GTC observations. The likely pulsar companion is shown in black.

First, the source colour is also in agreement with that of red/brown dwarfs that are cool low-mass ($M \sim$ 0.08–0.6 $M_\odot$) main-sequence stars. According to the correlation between the colour and the spectral type, based on the SDSS sample of M, L, and T dwarfs (Hawley et al. 2002), the source can be an M0–M3V red dwarf or a T-type brown dwarf. The corresponding distance of a red dwarf is $\gtrsim$8 kpc, and the object with $b = +29.6$ deg (see Table 1) must be located at $\gtrsim$4 kpc above the Galactic disc. A T-type brown dwarf would be very close to the Sun at a distance $\lesssim$50 pc. Both values are not consistent with the distance to J0740 and, in this case, the source must be rejected as the MSP companion.

Another possibility is that the source is a red subdwarf. Red subdwarfs are the metal-poor analogues of late-type dwarfs (see e.g. Zhang et al. 2013; Savcheva, West & Bochanski 2014). Absolute magnitudes of most of the detected late-type subdwarfs are $9 \lesssim M_{r'} \lesssim 14$, which infer a distance of $\gtrsim$3 kpc to the source. This is also incompatible with the distance to J0740 and implies the object is outside the Galactic disc.

Finally, the extragalactic origin of the source cannot be excluded. The total Galactic extinction in this direction $E_{B-V} \lesssim 0.06$ is relatively low and such colour is expected, e.g. for distant E/S0/Sbc-type galaxies with redshifts $z \leq 1$ (see e.g. Georgakakis, Georgantopoulos & Akylas 2006).

If the source is not related to the J0740, we can consider the derived magnitudes as lower limits for the pulsar binary companion. In this case it could be even cooler and older though we cannot determine the type of its atmosphere. Deep infrared observations are necessary to clarify the properties and nature of the detected source. For a cool WD with a pure helium atmosphere one can expect the BB-like spectral energy distribution. Future proper motion measurements can confirm the association of the likely counterpart with J0740.

ACKNOWLEDGEMENTS

We thank the anonymous referee for useful comments and Pierre Bergeron for helpful discussions. The work of DMB, AVK, and DAZ (Sections 2 and 3) was supported by the Russian Foundation

for Basic Research, project No. 18-32-00781 mol_a. AYuK and SVZ acknowledge PAPIIT grant IN-100617 for resources provided towards this research. The work is based on observations made with the Gran Telescopio Canarias (GTC), installed at the Spanish Observatorio del Roque de los Muchachos of the Instituto de Astrofísica de Canarias, in the island of La Palma. IRAF is distributed by the National Optical Astronomy Observatory, which is operated by the Association of Universities for Research in Astronomy (AURA) under a cooperative agreement with the National Science Foundation. This work has made use of data from the European Space Agency (ESA) mission *Gaia* (https://www.cosmos.esa.int/gaia), processed by the *Gaia* Data Processing and Analysis Consortium (DPAC, https://www.cosmos.esa.int/web/gaia/dpac/consortium). Funding for the DPAC has been provided by national institutions, in particular the institutions participating in the *Gaia* Multilateral Agreement. DAZ thanks Pirinem School of Theoretical Physics for hospitality.

REFERENCES

Abolfathi B. et al., 2018, ApJS, 235, 42
Alpar M. A., Cheng A. F., Ruderman M. A., Shaham J., 1982, Nature, 300, 728
Althaus L. G., Miller Bertolami M. M., Córsico A. H., 2013, A&A, 557, A19
Antoniadis J. et al., 2013, Science, 340, 448
Archibald A. M. et al., 2009, Science, 324, 1411
Archibald A. M. et al., 2018, Nature, 559, 73
Arzoumanian Z. et al., 2018, ApJS, 235, 37
Backer D. C., Kulkarni S. R., Heiles C., Davis M. M., Goss W. M., 1982, Nature, 300, 615
Bassa C. G., van Kerkwijk M. H., Kulkarni S. R., 2006, A&A, 450, 295
Bassa C. G. et al., 2014, MNRAS, 441, 1825
Bassa C. G., Antoniadis J., Camilo F., Cognard I., Koester D., Kramer M., Ransom S. R., Stappers B. W., 2016, MNRAS, 455, 3806
Becker W., Kramer M., Sesana A., 2018, Space Sci. Rev., 214, 30
Bergeron P. et al., 2011, ApJ, 737, 28
Bisnovatyi-Kogan G. S., Komberg B. V., 1974, Sov. Astron., 18, 217
Cadelano M., Pallanca C., Ferraro F. R., Salaris M., Dalessandro E., Lanzoni B., Freire P. C. C., 2015, ApJ, 812, 63
Cordes J. M., Lazio T. J. W., 2002, preprint (arXiv:astro-ph/0207156)
Dai S., Smith M. C., Wang S., Okamoto S., Xu R. X., Yue Y. L., Liu J. F., 2017, ApJ, 842, 105
Drimmel R., Cabrera-Lavers A., López-Corredoira M., 2003, A&A, 409, 205
Freire P. C. C. et al., 2017, MNRAS, 471, 857
Gaia Collaboration, 2016, A&A, 595, A1
Gaia Collaboration, 2018, A&A, 616, A1
Georgakakis A. E., Georgantopoulos I., Akylas A., 2006, MNRAS, 366, 171
Gianninas A., Curd B., Thorstensen J. R., Kilic M., Bergeron P., Andrews J. J., Canton P., Agüeros M. A., 2015, MNRAS, 449, 3966
Green G. M. et al., 2018, MNRAS, 478, 651
Guillemot L. et al., 2016, A&A, 587, A109
Hall P. B., Kowalski P. M., Harris H. C., Awal A., Leggett S. K., Kilic M., Anderson S. F., Gates E., 2008, AJ, 136, 76
Hawley S. L. et al., 2002, AJ, 123, 3409
Holberg J. B., Bergeron P., 2006, AJ, 132, 1221
Istrate A. G., Tauris T. M., Langer N., Antoniadis J., 2014, A&A, 571, L3
Istrate A. G., Marchant P., Tauris T. M., Langer N., Stancliffe R. J., Grassitelli L., 2016, A&A, 595, A35
Jacoby B. A., Hotan A., Bailes M., Ord S., Kulkarni S. R., 2005, ApJ, 629, L113
Karpova A. V., Zyuzin D. A., Shibanov Y. A., Kirichenko A. Y., Zharikov S. V., 2018, PASA, 35, e028
Kilic M., 2011, in Hoard D. W., ed., White Dwarf Atmospheres and Circumstellar Environments. Wiley-VCH, Weinheim, p. 25
Kilic M., Thorstensen J. R., Kowalski P. M., Andrews J., 2012, MNRAS, 423, L132
Kirichenko A. Y., Zharikov S. V., Zyuzin D. A., Shibanov Y. A., Karpova A. V., Dai S., Cabrera Lavers A., 2018, MNRAS, 480, 1950
Kowalski P. M., Saumon D., 2006, ApJ, 651, L137
Kramer M., 2018, in Weltevrede P., Perera B. B. P., Preston L. L., Sanidas S., eds, IAU Symp. S337, Pulsar Astrophysics the Next Fifty Years. Cambridge University Press, Cambridge, UK, p. 128
Laffon H., Smith D. A., Guillemot L., for the Fermi-LAT Collaboration, 2015, Fermi Symp. proc., eConf C141020.1, preprint (arXiv:1502.03251)
Landolt A. U., 1992, AJ, 104, 340
Lattimer J. M., 2012, Ann. Rev. Nucl. Part. Sci., 62, 485
Lindegren L. et al., 2018, A&A, 616, A2
Lorimer D. R., Kramer M., 2012, Handbook of Pulsar Astronomy. Cambridge Univ. Press, Cambridge
Lynch R. S. et al., 2018, ApJ, 859, 93
Manchester R. N., 2017a, J. Astrophys. Astron., 38, 42
Manchester R. N., 2017b, J. Phys.: Conf. Ser., 932, 012002
Nicastro L., Lyne A. G., Lorimer D. R., Harrison P. A., Bailes M., Skidmore B. D., 1995, MNRAS, 273, L68
Nice D. J., Taylor J. H., 1995, ApJ, 441, 429
Oppenheimer B. R. et al., 2001, ApJ, 550, 448
Papitto A. et al., 2013, Nature, 501, 517
Prager B. J., Ransom S. M., Freire P. C. C., Hessels J. W. T., Stairs I. H., Arras P., Cadelano M., 2017, ApJ, 845, 148
Reid M. J. et al., 2014, ApJ, 783, 130
Rivera-Sandoval L. E. et al., 2015, MNRAS, 453, 2707
Roy J. et al., 2015, ApJ, 800, L12
Savcheva A. S., West A. A., Bochanski J. J., 2014, ApJ, 794, 145
Schlafly E. F., Finkbeiner D. P., 2011, ApJ, 737, 103
Shapiro I. I., 1964, Phys. Rev. Lett., 13, 789
Shklovskii I. S., 1970, Sov. Astron., 13, 562
Smith J. A. et al., 2002, AJ, 123, 2121
Stovall K. et al., 2014, ApJ, 791, 67
Swihart S. J. et al., 2018, ApJ, 866, 83
Tauris T. M., 2011, in Schmidtobreick L., Schreiber M. R., Tappert C., eds, ASP Conf. Ser. Vol. 447, Evolution of Compact Binaries. Astron. Soc. Pac., San Francisco, p. 285
Tremblay P.-E., Bergeron P., Gianninas A., 2011, ApJ, 730, 128
van Kerkwijk M. H., Bassa C. G., Jacoby B. A., Jonker P. G., 2005, in Rasio F. A., Stairs I. H., eds, ASP Conf. Ser. Vol. 328, Binary Radio Pulsars. Astron. Soc. Pac., San Francisco, p. 357
van Oirschot P., Nelemans G., Toonen S., Pols O., Brown A. G. A., Helmi A., Portegies Zwart S., 2014, A&A, 569, A42
Weisberg J. M., Huang Y., 2016, ApJ, 829, 55
Yao J. M., Manchester R. N., Wang N., 2017, ApJ, 835, 29
Zhang Z. H. et al., 2013, MNRAS, 434, 1005

This paper has been typeset from a TEX/LATEX file prepared by the author.